Science of Remote Sensing 5 (2022) 100042

Contents lists available at ScienceDirect

Science of Remote Sensing

journal homepage: www.sciencedirect.com/journal/science-of-remote-sensing

# Carbon fluxes from contemporary forest disturbances in North Carolina evaluated using a grid-based carbon accounting model and fine resolution remote sensing products

Weishu Gong [a,*], Chengquan Huang [a], Richard A. Houghton [b], Alexander Nassikas [b], Feng Zhao [a], Xin Tao [c], Jiaming Lu [a], Karen Schleeweis [d]

[a] Department of Geographical Sciences, University of Maryland, College Park, United States
[b] Woodwell Climate Research Center, United States
[c] Department of Geography, University at Buffalo, United States
[d] USDA Forest Service, United States

ARTICLE INFO

*Keywords:*
Carbon fluxes
LULCC
Houghton's bookkeeping model
Spatial-explicit carbon flux model
Spatial and temporal patterns of carbon fluxes

ABSTRACT

Land use/land cover change is a key component in terrestrial carbon cycle, yet there are still large uncertainties in the terrestrial carbon budget. To reduce such uncertainties and refine the spatial distribution of carbon flux, a 30-m Grid-based Carbon Accounting (GCA) model was proposed. We adapted a well-established bookkeeping model into a spatial-explicit model to utilize Landsat time series stacks and to calculate the carbon fluxes resulting from three types of forest disturbances including forest harvesting, forest-to-urban conversion, and fire. Our model results provide spatial details at sub-ha scale that are crucial for carbon management at individual landowner levels. Sensitivity analysis revealed that both pre-disturbance forest carbon and disturbance intensity had large impact on carbon flux estimates arising from forest disturbances that occurred between 1986 and 2010 in North Carolina. At the state level, forest harvesting and fire from 1986 to 2010 released 88.5 MT and 1.6 MT carbon respectively. During the same period, regrowing trees over the logged area absorbed 142.7 MT carbon while those over burned area absorbed 1.6 MT more. The net flux from harvesting, fire, and post-disturbance growth was −52.5 MT. Conversion of forest to urban resulted in a net source of 5.3 MT. Overall, the areas subject to the three types of disturbances and post-disturbance growth was a net sink of 47.2 MT carbon over the entire study period. While our modeling framework was tested at the 30 m spatial resolution in this study, it can be adapted for use with finer spatial and/or temporal resolution remote sensing products that will become more readily available in the coming years, thus further improve the carbon flux estimates.

## 1. Background

The past century has seen a rise in atmospheric CO2 concentration that leads to the observed global climate change (IPCC, 2014). To combat it, numerous carbon emission reduction initiatives, such as REDD+ ("reducing emissions from deforestation and forest degradation", and the + standing for "the role of conservation, sustainable management of forests and enhancement of forest carbon stocks") and various carbon trade/carbon credit programs have been established (Agrawal et al., 2011; Canadell and Raupach, 2008; Denise et al., 2011; Schulze et al., 2002). This calls for robust carbon accounting systems to support the measurement, reporting, and verification (MRV) of carbon pools and fluxes (Birdsey et al., 2006; Fahey et al., 2010; Lamb et al., 2021), yet large uncertainties exist in current estimates of carbon fluxes between the biosphere and the atmosphere (Houghton, 2013; Antonarakis, 2014). The most recent global carbon budget reports emissions from land-use change at around 1.3 ± 0.7 GtC $yr^{-1}$ over the 1970–1999 period, and 0.9 ± 0.7 GtC in 2020 (Friedlingstein et al., 2021): the uncertainty is over 50% of the estimated flux. An accurate estimation of the Earth's carbon budget is crucial for national and international decision makers when considering climate mitigation strategies (Griscom et al., 2017; Marland et al., 2003; Noormets et al., 2015), thus reducing such uncertainties is of great interest in the scientific community, especially in quantifying carbon fluxes at more local and regional scales (Turner

* Corresponding author.
*E-mail address:* wsgong@umd.edu (W. Gong).

https://doi.org/10.1016/j.srs.2022.100042
Received 30 October 2021; Received in revised form 28 January 2022; Accepted 10 March 2022
Available online 24 March 2022

et al., 2016).

There are many ways to estimate forest carbon pools and fluxes. The first one is the inverse models used with variations in atmospheric concentrations of CO2 to infer sources and sinks (Fan et al., 1998; Pacala et al., 2001; Crevoisier et al., 2007). These studies have generally estimated larger net sinks than other approaches, but the uncertainties are high. The second approach is to use process-based ecosystem models or terrestrial biosphere models (TBMs) to simulate changes in carbon storage on land (e.g. Tian et al., 1999; Hurtt et al., 2002; Williams et al., 2020). The estimates of annual NEP from TBMs are also highly variable, for example, the estimates of annual NEP for temperate North America varies from a sink of 1600 to a source of 500 TgC/yr for the period 2000–2005 (Huntzinger et al., 2012). The major components of NEP (GPP and Rs) varied even more than NEP among the models. The third approach relies on data from forest inventories to calculate carbon budgets (Birdsey and Heath, 1995; Turner et al., 1995; Smith et al., 2007; Pan et al., 2011; Gray and Whittier, 2014). Estimates from inventory data are less variable than estimates from inverse studies and ecosystem models, and generally the estimated net carbon sink in forests is also smaller. But the strategic national inventory data are based on sampling strategies designed primarily to estimate stocks (growth and mortality), not to monitor changes in area at fine spatial resolution (Bradford et al., 2010). The fourth approach is to utilize carbon accounting methods to track carbon fluxes arising from land use conversion, forest harvest, wildfire, and other land use/land cover change types (Houghton et al., 1999; Zheng et al., 2011; Brack and Richards, 2002). Driven by tabular statistics on land use change and related carbon pools, this approach typically produces results with spatial characteristics no better than those of the tabular input data. Such results might be useful at national or regional levels, but lack the spatial details needed to support carbon management decision makings by local agencies or individual landowners. The carbon flux estimates from different approaches vary greatly, even the direction of the flux can differ at global scale, either due to incomplete accounting inherent in some of the methods (Houghton, 2003a) or data variability (Huntzinger et al., 2012). But with spatially detailed land-use change and disturbance records, such differences may be resolved (Houghton, 2003a).

Deriving carbon estimates with needed spatial details was difficult in the past, partly because spatial products on the required model inputs did not exist. With rapid advances in remote sensing technology, however, it has become increasingly more feasible to map many variables important for tracking carbon fluxes with increasingly better quality (Goward et al., 2008). Landsat images have been used to map land cover and land cover/land use change for decades (Powell et al., 2010; Schroeder et al., 2014). Following the opening of the entire Landsat archive for no-cost access, the multi-decade Landsat record has been used to nationally reconstruct forest disturbance history (Goward et al., 2010; Huang et al., 2010), map disturbance agent (Schleeweis et al., 2020; Schroeder et al., 2014), and quantify disturbance intensity (Tao et al., 2019). Integration of remote sensing observations with field plot data and/or other measurements allowed derivation of biomass products at local, national, to continental scales (Hall et al., 2006; Santi et al., 2017). With increasingly more optical, radar, and lidar observations provided by existing and forthcoming satellite missions, including Sentinel-1 and -2, the Ice, Cloud and land Elevation Satellite (ICESAT-2), and Global Ecosystem Dynamics Investigation (GEDI) mission, the ability to produce high quality data products on land change, biomass density, and other biophysical variables needed to calculate terrestrial carbon fluxes will continue to improve (Xiao et al., 2019).

Effective use of the rich, remote sensing-based datasets to advance carbon management decision making requires a framework to integrate these datasets with models to produce carbon estimates with required spatial-temporal details. A major goal of this study was to develop a grid-based framework where fine resolution disturbance, forest carbon, and other remote sensing products can be used as inputs to a well-established carbon accounting model (Houghton et al., 1999), which has been used in varies studies including past Global Carbon Budget (Le Quéré et al., 2016; Friedlingstein et al., 2021) and tracks carbon fluxes through several different pool, to produce spatially detailed map products of carbon pools and fluxes. Previous studies have shown that this can lead to better estimations of carbon fluxes where regional statistics are unavailable, or when close examination of spatial patterns are needed (DeFries et al., 2002; Kuemmerle et al., 2011; Tang et al., 2020). Here in this study, we have established a framework that provides yearly estimates of carbon fluxes resulting from forest disturbances at a fine resolution of 30-m. We have tested this framework over North Carolina where detailed forest carbon and Landsat-based disturbance products are available and used it to produce 30-m map products of carbon fluxes arising from forest disturbances occurred between 1986 and 2010. These fine resolution map products are valuable for understanding the spatial-temporal patterns of carbon sources from forest disturbances and sinks from post-disturbance growth. More importantly, they can provide much needed details that are mostly unavailable thus far for carbon accounting, management, and related decision support at individual property owner, municipal, county, or even state levels.

## 2. Methods

### 2.1. Study area and period

North Carolina is located in the southeastern United States. It is split between two ecozones, Zone 21, subtropical humid forest, and Zone 35, temperate mountain system (Fig. 6). Its 100 counties are distributed from the Atlantic coast in the east to the Great Smoky Mountains in the west. About 60% (75199.3 $km^2$) of the state's 139,390 $km^2$ land base is forest land (Brown et al., 2014), most of which is classified as timberland (Bardon et al., 2010). Major forest type groups include Oak-Hickory, Loblolly-shortleaf pine, Oak-pine, and Oak-Gum-Cypress. More than half of the state's forests were disturbed at least once between 1985 and 2010 (Huang et al., 2015). While timber harvest is the dominant disturbance type, damages from hurricane, insect outbreak, snow/ice, fire, and other natural disturbances are also common. The state's total area subject to stand clearing disturbances was relatively stable, but the impact of partial disturbances had large inter-annual variability (Tao et al., 2019). In this study, we ran the model for the period of 1986–2010. Note that any latency effect from disturbances before 1986 was not calculated, nor was carbon absorption from undisturbed pixels included in the model results reported in this study.

### 2.2. The original bookkeeping carbon accounting (BCA) model

The Bookkeeping Carbon Accounting (BCA) model (Houghton et al., 1999) is a well-established model for tracking carbon fluxes arising from land use and land cover change. This model divides the globe into ecozones following the Food and Agriculture Organization of the United Nations (FAO) Global Ecological Zones (GEZ, second edition). For each ecozone, the BCA model keeps track of the carbon in four major pools: living aboveground and belowground biomass; dead biomass, including coarse woody debris; harvested wood products; and soil organic carbon (Houghton and Nassikas, 2017). These major pools are divided into smaller categories for calculation purposes: soil release and uptake, slash (woody debris left on site), carbon burned on site, regrowth after disturbance, and decay of various industrial wood products. Carbon pools and the fluxes for different disturbance types are tracked at the ecozone level. Table 1 lists the forest change processes and carbon pools considered in this study, and the key parameters used to calculate these pools and fluxes are listed in Table 2.

For a disturbance event that resulted in a disturbance area of LC, the release from the carbon ended up in the slash in any given year X is

$$\text{Slash}_r \text{ in X} = (\text{Slash Pool}_{X-1} + LC * C_{Prim} * F_{Slash}) * (1 - e^{-DRslash}) \quad (1)$$

**Table 1**
Pools tracked by the BCA model for LULCC types considered in this study (indicated by "X").

| | Fire | Wood Harvesting | Conversion to Urban Land |
|---|---|---|---|
| Soil Release | | | |
| Soil Uptake | | | |
| Slash | X | X | |
| Burned | X | | X |
| Regrowth | X | X | |
| Wood Products | | X | |

**Table 2**
Ecozone-specific parameters used by the BCA model.

| Name | Unit | Description |
|---|---|---|
| $C_{Prim}$ | g/Ha | Carbon density in undisturbed, mature/primary forest |
| $C_{Min}$ | g/Ha | Minimum carbon density after disturbance |
| $C_{Sec}$ | g/Ha | Carbon density in recovered, secondary forest |
| $F_{Slash}$ | | Fraction of carbon ended up in slash pool |
| $DR_{Slash}$ | | Decay rate coefficient for slash pool |
| $F_{P1}$ | | Fraction of carbon ended up in 1-year decay pool |
| $F_{P10}$ | | Fraction of carbon ended up in 10-year decay pool |
| $F_{P100}$ | | Fraction of carbon ended up in 100-year decay pool |
| $T_{ms}$ | Year | Time for forest to grow into secondary forest from stand-clearing disturbance |
| $T_{sp}$ | Year | Time for forest to grow into mature forest from secondary forest |

And the carbon pool after each year's release is

$$\text{Slash Pool in X} = (\text{Slash Pool}_{X\text{-}1} + LC * C_{Prim} * F_{Slash}) * e^{-DRslash} \quad (2)$$

The carbon burned on site is released immediately in the year of disturbance, and can be calculated as

$$P_{1r} = LC * F_{P1} * (C_{Prim} - C_{Min}) \quad (3)$$

For regrowth after disturbance, it is assumed that the growth rate is fast when the disturbed land is recovering from minimum to secondary forest, then the rate becomes slow until the forest reaches mature stage, at which point the growth stops. During each regrowth stage, it is assumed that the growth rate is constant. The annual carbon uptake or sink by regrowth from minimum to secondary forest and from secondary forest to mature forest are calculated using equations (4) and (5)

$$\text{Regrowth}_{min2sec} = LC * (C_{Sec} - C_{Min}) / T_{ms} \quad (4)$$

$$\text{Regrowth}_{sec2mat} = LC * (C_{Mat} - C_{Sec}) / T_{ms} \quad (5)$$

The total annual uptake by regrowth is the sum of annual uptake by regrowth from all previous disturbances.

For the wood products, based on different product types, the pool is divided into a fast decay pool (10-year decay pool, or P10, e.g., paper products) and a slow decay pool (100-year decay pool, or P100, e.g., furniture, wood used in buildings). The calculations for these pools and their annual releases are similar to Eq. (1) and Eq. (2), where 1/10th or 1/100th of the respective pool is released per year.

### 2.3. Development of a grid-based carbon accounting (GCA) model

A major limitation of the current BCA model is its inability to provide results at a resolution required for project level or landscape level carbon management. To overcome this problem, we reimplemented the BCA model within a gridded framework to leverage the increasingly more available remote sensing products that could be used to derive the parameters required by the model. In this framework, a study area is divided into even-sized grid cells (e.g., 30-m pixels). Carbon pools and fluxes are calculated for individual grid cell instead of ecozones. For each cell, the parameters that can be derived from available remote sensing products will have cell-specific values derived from those products. The remaining parameters will inherit the ecozone-based values from the original BCA model according to which ecozone that cell belongs to.

As will be discussed in section 2.3, several remote sensing products were available over the study area, including 1) a carbon content map, and 2) a suite of disturbance products providing details on the timing/year, intensity, as well as type/attribution of each disturbance event. With these products, the GCA model was implemented such that it could account for carbon fluxes arising from multiple disturbance events that occurred within the same grid cell in different years. Further, we used these products to improve the calculation of carbon fluxes arising from disturbance and post-disturbance regrowth through the following steps:

First, the carbon density map was used to replace $C_{Prim}$ in determining the initial carbon density of a grid cell right before the first disturbance event was detected at that location (pre-disturbance carbon density). Second, the amount of carbon removed from the living biomass within that grid cell due to the first disturbance event was calculated as the product of pre-disturbance carbon density and the percentage of carbon removed (PCR) by that event, which was assumed to be 100% (stand clearing) when not using the disturbance intensity data. As will be discussed in section 2.4.1, the disturbance intensity products provided estimates of percent basal area removal (PBAR), which was the percentage of the total basal area of live trees removed by a disturbance event. Based on the allometric equations of Jenkins et al. (2003), which were developed to convert tree diameter measurements to biomass, the percentage of carbon removed (PCR) by a disturbance event can be calculated from PBAR using the following equation:

$$PCR = PBAR^{6/5}$$

Third, whether to use equation (4) or (5) to calculate the initial growth immediately following that disturbance event was determined according to the remaining carbon in live biomass after that event, which was the difference between pre-disturbance density and the amount of carbon removed by that event as calculated above. If the remaining carbon is below $C_{Sec}$, equation (4) is used. Otherwise, use equation (5).

Finally, if more disturbances were detected after the first disturbance over a pixel location, the pre-disturbance carbon density for each subsequent disturbance event was calculated as the sum of the remaining carbon after the previous disturbance and the carbon accumulated through the growth calculate in the third step. The fluxes arising from disturbance and post-disturbance growth were then calculated following the second and third steps.

### 2.4. Model inputs

Since the GCA model was in essence a reimplementation of the BCA model within a gridded framework, most of its parameters would have values equivalent to those used in the original BCA model. That is, for each of those parameters, all grid cells in the GCA model that were located within the same ecozone of the BCA model had the same ecozone-based values used by the original BCA model. For the parameters that could be derived from available remote sensing products, their values over each grid cell will be derived from remote sensing products and can vary within the ecozones. The remote sensing products used in this study included a suite of forest disturbance maps and a pre-disturbance carbon density map all scaled to 30 m resolution.

#### 2.4.1. Forest disturbance data

Several products were used to produce a disturbance dataset with information on the timing (year), type (attribution), and intensity of disturbances that occurred in North Carolina from 1985 to 2010. The first were annual forest disturbance maps showing which pixels had

disturbances in what years (Huang et al., 2015). These maps were derived using Landsat time series stacks (LTSS) (Huang et al., 2009) and the vegetation change tracker (VCT) algorithm (Huang et al., 2010). For each disturbance event detected by the LTSS-VCT approach, if it was also mapped as a burned pixel by the annual fire maps derived through the Monitoring Trends in Burn Severity (MTBS) project (Eidenshink et al., 2007), then it was a fire disturbance. Otherwise it was a wood harvesting event unless it was classified as a conversion to urban as follows – if at least one disturbance was detected at a pixel location and that pixel was mapped as an urban pixel in 2011 by the National Land Cover Dataset (NLCD 2011) (Homer et al., 2015), then the last disturbance detected over that pixel was a conversion to urban. We used the NLCD 2011 because it represents land covers in the study area closest to the end of our study period, thus can help classifying disturbance types the most accurately compared to NLCD from other years. It should be noted that if two or more disturbance events were detected over the same pixel location, each event could be of a different type. However, if one of the types was a conversion to urban, that type must be the last one, because wood harvesting or fire could not happen over an area already converted to urban. The decision process used to attribute the detected disturbances is shown in Fig. 1.

For each disturbance event determined above, its intensity was derived based on the PBAR dataset produced by (Tao et al., 2019). As mentioned earlier, PBAR was a measure of the percentage of total live tree basal area that was removed by a disturbance event. The PBAR value for a disturbance event was derived based on the spectral change values associated with that disturbance event and a model calibrated using reference PBAR data calculated from pre- and post-disturbance field measurements collected through the USFS Forest Inventory and Analysis (FIA) program. While in the Tao et al. (2019) study, PBAR was calculated without considering the disturbance type, for this study, the PBAR values were set to 100% for all conversion-to-urban disturbances.

#### 2.4.2. Pre-disturbance carbon density data

As mentioned in section 2.2, pre-disturbance carbon density – the carbon density at a pixel location right before a disturbance event, is required for calculating the carbon change arising from that event. Since disturbances could and did occur throughout the entire observing period, this would require annual carbon density maps for the entire study period, which unfortunately do not exist. Although there are at least two CONUS-wide carbon density maps (Kellndorfer et al., 2013; Wilson et al., 2013), the values from those maps could not be used because the pre-disturbance carbon density for disturbances occurred before the derivation of those maps. Here in this paper, we used the carbon density map developed by Wilson et al. (2013) as part of the model input. Assuming that harvesting is more likely to occur in older forests than younger ones, we applied a spatial filtering method to the Wilson map to derive a pre-disturbance carbon density map that might provide more realistic values than the values in the original maps or the ecozone level values used by the original BCA model. Specifically, for any pixel location, we calculated the 95 or 99 percentile value with a relatively large area surrounding that pixel, say a 6 km by 6 km window, and used that value as the pre-disturbance carbon density value for that location.

To evaluate how realistic the pre-disturbance carbon density values derived this way were, we selected the FIA plots that had field measurements right before they were disturbed in the VCT products and plotted the FIA-based pre-disturbance carbon values against those from the original carbon density map as well as the pre-disturbance carbon density maps derived above. Fig. 2 shows that the median values from the pre-disturbance maps derived using both 95 and 99 percentiles were more realistic and closer to the 1:1 line compared to FIA measurements than that derived from the original carbon map, demonstrating that the spatial filtering method did provide more realistic pre-disturbance carbon density values.

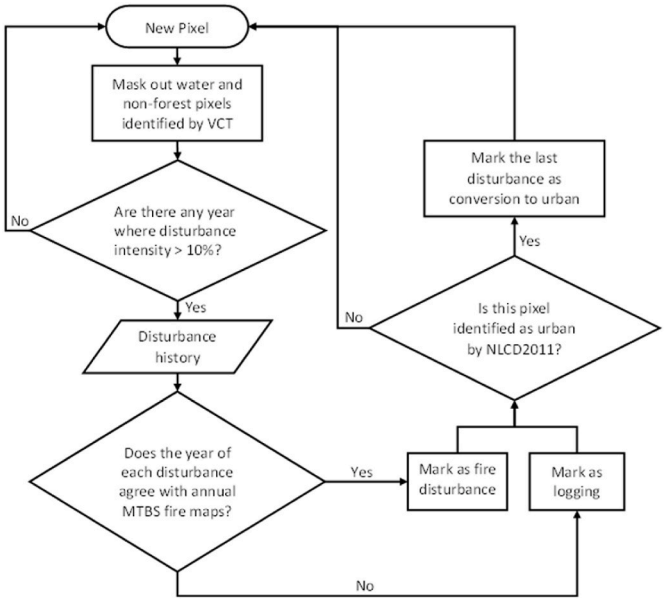


**Fig. 1.** The process of determining disturbance attribution.

#### 2.4.3. Other inputs

We used the pre-set parameter values provided with the original bookkeeping model for all other inputs. Attempts were made to find better forest growth rates with FIA plot data, however they vary greatly among different plots, even in the same ecozone (Fig. 3), with the average growth rate far larger than the median in each ecozone (Table 3). There are many factors that affect growth rates of trees, including but not limited to age, nutrient availability, climate, and species, and it is difficult to determine reasonable growth rates for each ecozone to use in the bookkeeping model with currently available data, so the original parameter values were used in the end.

### 2.5. Carbon modeling scenarios

The ability of the GCA model to use spatially explicit remote sensing products made it possible to assess the impact of those inputs on carbon estimates at finer spatial scales. In this study, four scenarios were designed to evaluate the impact of the products described in section 2.4, (Table 4). In the first scenario, neither the disturbance intensity dataset nor the pre-disturbance carbon density dataset was used. Instead, pre-defined mature forest carbon density values were used as pre-disturbance carbon density and all disturbances were considered stand clearing according to the original model setting (OMS) of the BCA model. In scenario 2, only the spatial disturbance intensity (SDI) dataset was used. Pre-defined mature forest carbon density values were used as pre-disturbance carbon density values. In scenario 3, only the spatial pre-disturbance carbon density (SPC) dataset was used. All disturbances were assumed to be stand clearing. In the last scenario, both spatial datasets (SDI + SPC) were used. Assuming the remote sensing products would produce more realistic carbon estimates than using the original model parameters, the final carbon fluxes arising from the mapped disturbances were calculated using scenario 4 (SDI + SPC). The differences among the four scenarios could be used to examine the impact of the remote sensing products on the estimation of carbon fluxes arising from forest disturbances and recover in recent decades.

## 3. Results

### 3.1. Model verification and sensitivity analysis

The model was first coded following the logic and assumptions of the

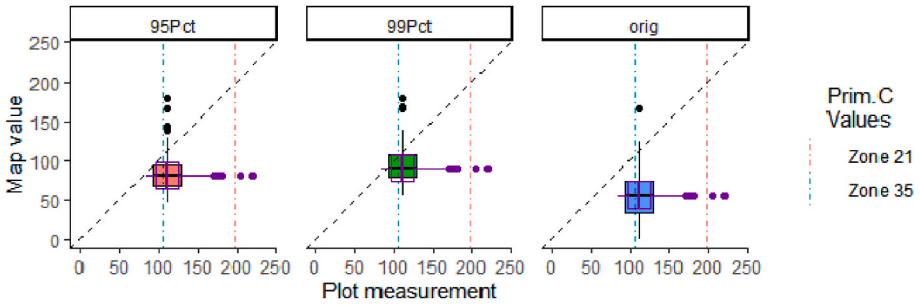


**Fig. 2.** Comparison of carbon density values between plot measurements and derived maps. After filtering the original map with 95th or 99th percentile in a 6 km by 6 km window, the range of values are closer to those of undisturbed plots.

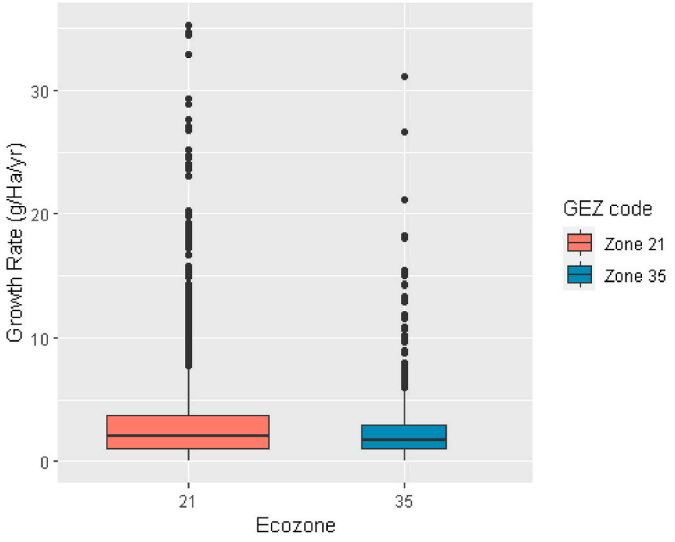


**Fig. 3.** Distribution of forest growth rates calculated from FIA plot data. The box widths are proportional to the square-root of the number of observations in each ecozone.

original BCA model, with every disturbance assumed to be stand-clearing, the initial carbon density right before the disturbance always at the mature forest level, and conversion to agricultural or urban land could happen multiple times on a pixel. With this intermediate model, not only the total net fluxes over the entire observing period but also the annual source and sink estimates for all major carbon pools derived using the two models were the same, demonstrating that we successfully deployed the BCA model in a gridded framework for producing spatially detailed carbon estimates. Then, the disturbance attribution process was improved to account for multiple disturbance events on the same pixel (see Fig. 1), disturbance intensity and starting carbon density were replaced by gridded data derived from satellite remote sensing products, and the carbon density throughout the disturbance-regrowth process was tracked in the finalized GCA model. The total fraction of disturbed forest pixels is about 44.7% in North Carolina, or 35874.3 $km^2$ out of all 82159.5 $km^2$ of total forested area.

Model results derived with and without using the spatially explicit pre-disturbance carbon density map and the disturbance intensity dataset as inputs to the GCA model show that modifying these inputs had large impact on carbon estimates. Compared to benchmark results derived using original model settings (the OMS scenario), the net carbon flux arising from mapped disturbances over North Carolina during the study period was reduced from 242.9 MT (net source) to 136.4 MT (net source) when only the spatial disturbance intensity (the SDI scenario) was used. The flux value became negative (net sink) when the pre-disturbance carbon density map was used but all disturbances were assumed stand clearing (the SPC scenario). The net flux was further reduced to −47.2 MT when both spatial maps were used (the SPC + SDI scenario) (see Fig. 4).

Because wood harvesting was the dominant disturbance type in the study region, the two spatial datasets had the largest impacts on harvest source calculations. Emission from wood harvesting was estimated at

**Table 4**
Scenarios for assessing model sensitivity to spatial carbon density and disturbance intensity data.

| Scenario | Pre-disturbance C value used | Disturbance intensity data used? |
|---|---|---|
| Original model setting (OMS) | Ecozone-specific constant | No |
| Spatial disturbance intensity only (SDI) | Ecozone-specific constant | Yes |
| Spatial Pre-disturbance C density only (SPC) | Spatial pre-disturbance C density map | No |
| SPC + SDI | Spatial pre-disturbance C density map | Yes |

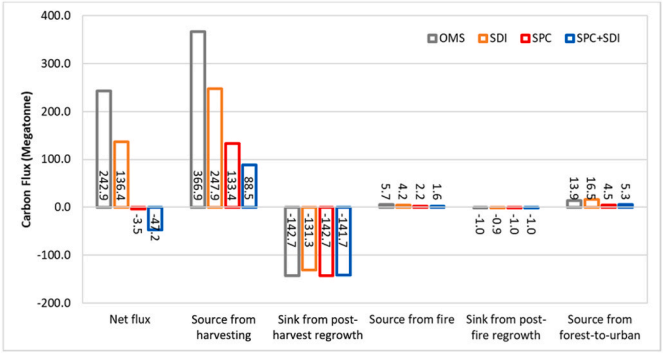


**Fig. 4.** Comparison of carbon fluxes by disturbance type between different scenarios. Using both RS-based carbon density map and disturbance intensity data has turned the 25-year net total C flux from source to sink.

**Table 3**
Growth rate statistics from selected FIA plots. The last two columns show the values provided with the original BCA model.

| GEZ code | count | median | avg | min | max | param_fastGR | param_slowGR |
|---|---|---|---|---|---|---|---|
| 21 | 3326 | 2.0876421 | 2.987681 | 0.001047 | 35.3077 | 2.96656 | 0.98884 |
| 35 | 919 | 1.7693155 | 2.514326 | 0.001976 | 64.1434 | 1.58216 | 0.52738 |

366.9 MT for the study region using the OMS scenario. It was reduced to 247.9 MT and 133.4 MT under scenarios SDI and SPC respectively, and further down to 88.5 MT when both datasets were used (the SPC + SDI scenario). The impacts of the two datasets on fire source estimates were similar but at much smaller scales because the total area affected by fire was only a small fraction of that subject to harvesting.

Driven by post-disturbance growth rates, sink calculation for both post-harvest and post-fire growth should not be directly affected by the two spatial datasets. However, because the model assumes a fast growth rate at relatively low carbon density and changes the growth rate to a lower value when a pixel's carbon density exceeds a threshold value, use of the two spatial datasets can affect a pixel's carbon value at any given time and hence can have indirect impact on the sink estimates for these post-disturbance growth processes.

While the impact of the pre-disturbance C dataset on source calculation for forest-to-urban conversion is similar to that for wood harvesting and fire events, the impact of the disturbance intensity dataset is more complicated. In theory, source calculation for forest-to-urban should not be affected by the disturbance intensity data, because the intensity should always be 100% for this change process. However, a pixel converted to urban could have one or more disturbances (mostly harvesting) prior to the final conversion to urban. For such a pixel, if a mature forest carbon value was assigned to it prior to its earliest disturbance event, a low disturbance intensity would result in a small carbon source and trigger the model to start calculating carbon increase from post-disturbance regrowth and the pixel's carbon density could exceed the assumed value for mature forest before the pixel was converted to urban. As a result, the source estimation for that forest-to-urban conversion event under the SDI scenario could be higher than that calculated under the OMS scenario. This could only happen to pixels that had other disturbances prior to the forest-to-urban conversion. This is why the annual forest-to-urban source values calculated under the OMS and SDI scenarios were similar in the first couple of years but differed in later years (Fig. 5(C)).

### 3.2. Carbon fluxes from disturbance and post-disturbance growth

Carbon fluxes arising from disturbances and post-disturbance growth over North Carolina were modeled using the SPC + SDI scenario where both the disturbance intensity and pre-disturbance carbon density datasets were used as inputs to the GCA model. Sources arising from harvesting, fire, and forest-to-urban conversion, as well as sinks from post-harvest and post-fire regrowth were calculated on an annual basis for every 30-m pixel that had at least one disturbance mapped. Fig. 6 shows the net flux images derived by summing up all source and sink terms over the study period for each pixel, along with a few full resolution zoom-in examples showing the fluxes driven by different change processes.

These 30-m maps can be aggregated for any geographic or administrative regions (e.g., areas affected by individual disturbance events, properties of individual landowners, districts, counties, and state) to derive estimates needed for addressing specific carbon management and/or decision support needs. At the state level, forest harvesting and fire from 1986 to 2010 released 88.5 MT and 1.6 MT carbon respectively. During the same period, regrowing trees over the logged area absorbed 142.7 MT carbon while those over burned area absorbed 1.6

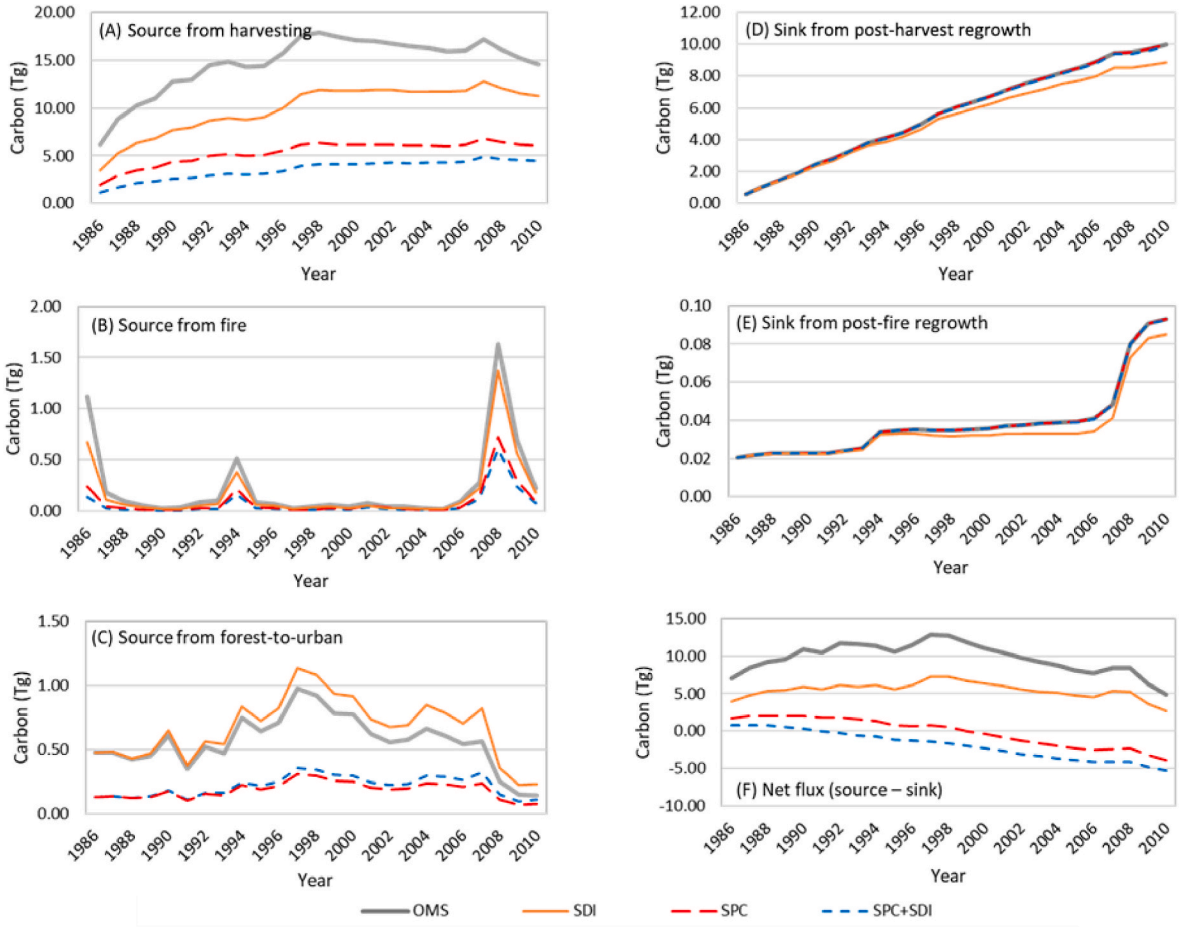


**Fig. 5.** Annual total carbon absorbed and released by disturbance types during the study period under the four different scenario settings. The trendlines show large differences among the sources under the four scenarios.

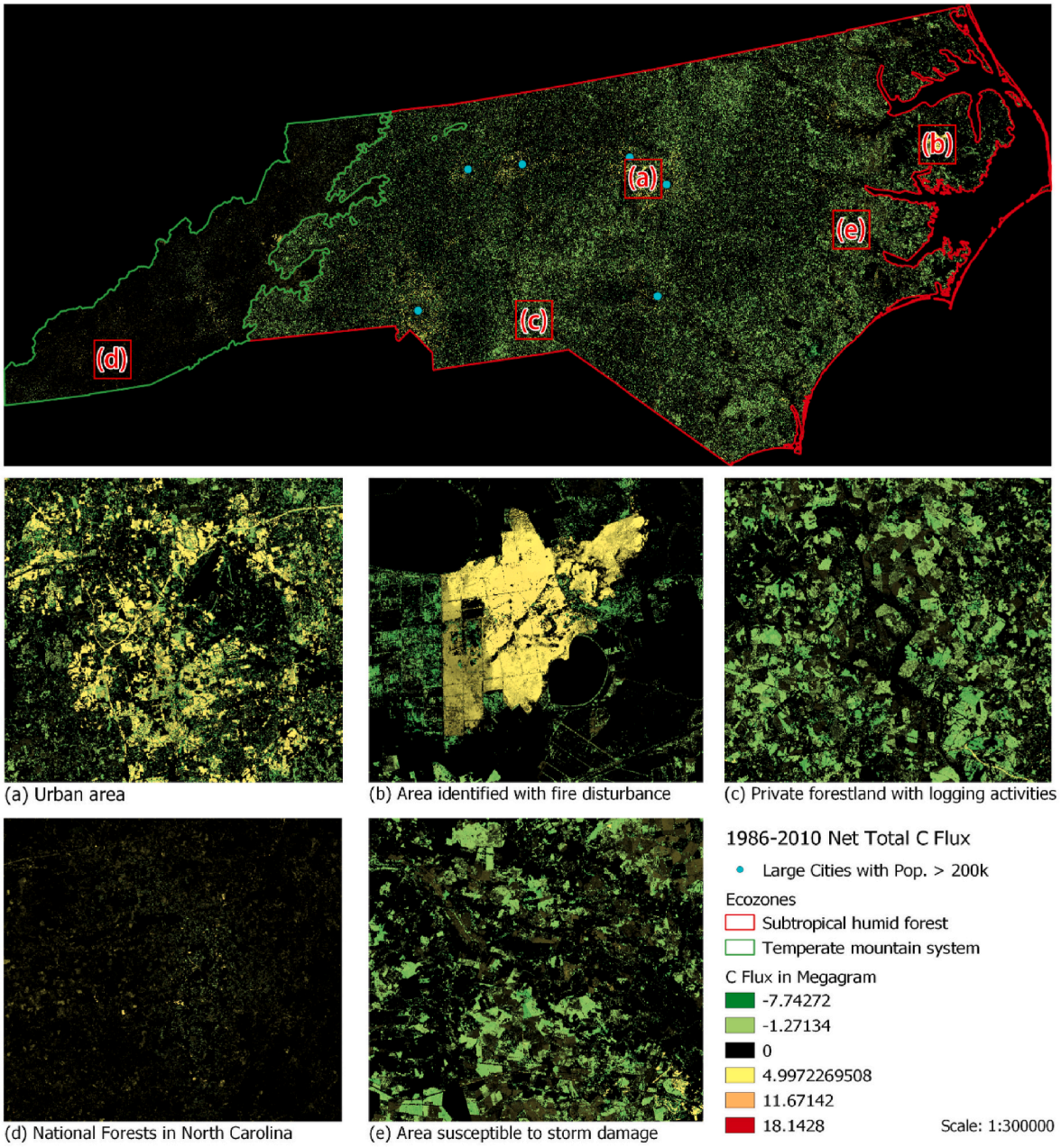


**Fig. 6.** A browse image of the 30-m net flux map derived by summing up all source and sink terms over the study period for each pixel. The full resolution zoom-in examples show the flux patterns over areas with (a) extensive forest-to-urban conversion, (b) a large fire occurred in 2008, (c) active wood harvesting followed by strong growth throughout the study period, (d) minimal disturbances within national park/national forests, and (e) storm damage/salvage logging followed by recovery.

MT more. The net flux from harvesting, fire, and post-disturbance growth was −52.5 MT. Conversion of forest to urban resulted in a net source of 5.3 MT. Overall, the areas subject to the three types of disturbances and post-disturbance growth was a net sink of 47.2 MT carbon over the entire study period.

The source and sink estimates differed substantially among the counties within the state (Fig. 7). Most counties with high carbon releases due to harvesting are located in the eastern side of the state, with Bertie and Beaufort having the highest releases. Except for Rutherford County and Wilkes County, harvesting emissions in most counties on the west side were only small fractions of many counties on the east side.

Emissions due to the other two disturbance types were small in general. However, each of the two disturbance types had some hotspots. As expected, counties surrounding population centers had higher emissions from urbanization, including the Mecklenburg County (the Charlotte metropolitan area), Wake County and Durham County (the Raleigh-Durham-Chapel Hill area, Fig. 7(A)), and Guilford County (suburban Greensboro). The few other counties that had sizable emissions from urbanization also had mid-sized cities (population >200k).

Large fire is not common in NC. In 2008, however, a fire ignited by lightning burned more than 41,500 acres, mostly within the Pocosin Lakes National Wildlife Refuge, resulting in high emissions in Tyrrell and Hyde counties. Several other counties, including Pender, Craven, and to lesser degrees, Burke and Washington, also had sizable emissions due to fire.

The carbon sink related to wood harvesting and fire is driven by post-disturbance growth. Given the fast forest growth rates in the study region (especially in ecozone 21), it does not take many decades for the

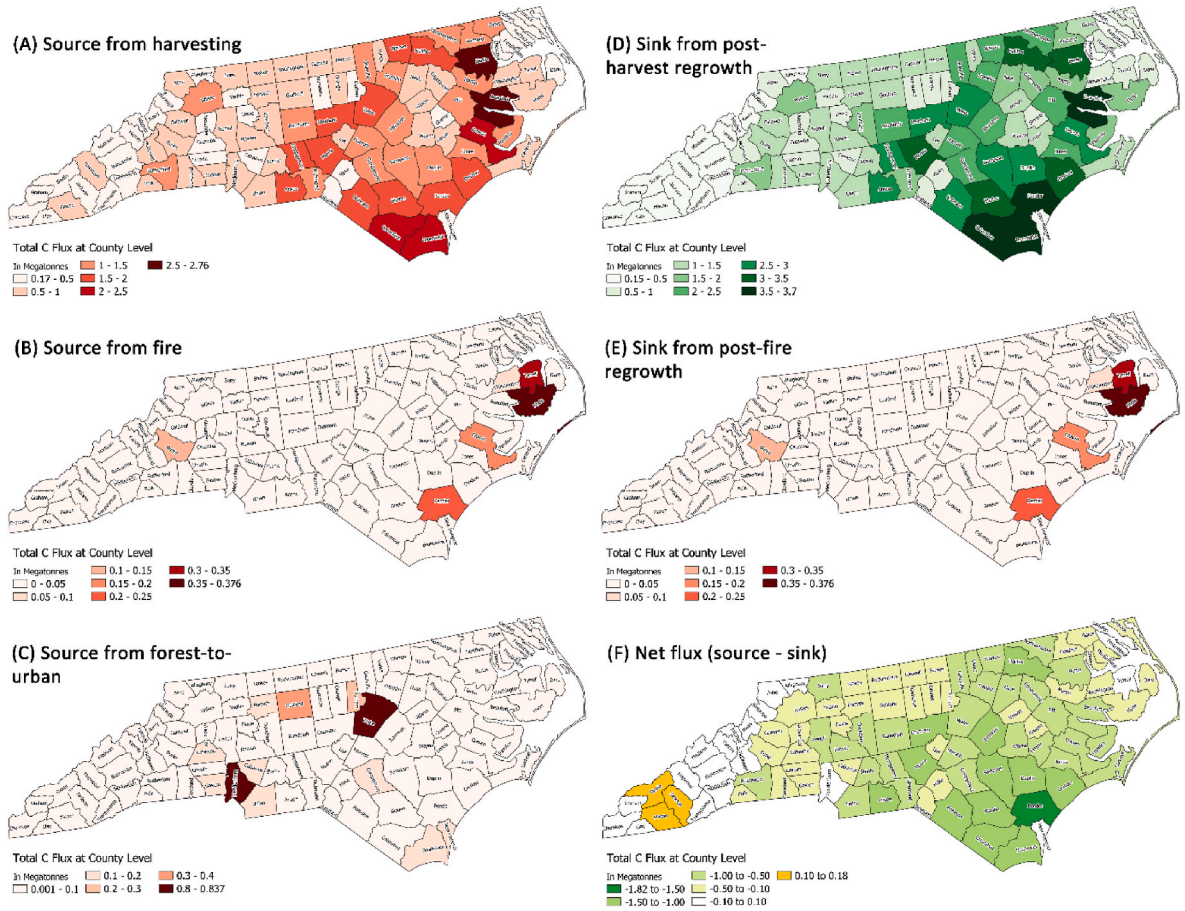


**Fig. 7.** Total carbon absorption and emission by disturbance types at county level during the 25-year study period. Wood harvesting activities are prevalent in the eastern part of the state, resulting in both large sources and sinks. Only a handful of counties are affected by fire. Emission from conversion to urban land is prominent in counties with major urban centers. Overall, the emission is less than or almost equal to the absorption in all counties.

carbon accumulation through post-disturbance growth to surpass the amount released by a disturbance event, especially when the pre-disturbance carbon is low or the intensity of that disturbance event is low, or both. As a result, most counties with high carbon releases due to wood harvesting had even higher sink values over the entire study period. These results, however, should not be considered as indicators that forests subject to wood harvesting might be a stronger carbon sink than undisturbed forests, as the latter was not considered in this study. Except for Pender County where the carbon sink from post-fire growth by 2010 exceeded the release from a fire occurred in 1986, the few counties that had fire disturbances had minimal sinks from post-fire growth.

Overall, the total c sink arising from post-disturbance recovery exceeded the total release from all three disturbance types in most counties in east and central North Carolina, resulting in negative net fluxes in those counties during the study period. The relatively large emissions from forest-to-urban conversion in Mecklenburg County and the 2008 Pocosin Lakes fire that spilled into Tyrrell County were offset by sinks from post-disturbance growth. As a result, the net fluxes from disturbance and post-disturbance growth were near zero in both counties. Three other counties in the east along with more than a dozen counties in the west also had near zero net fluxes. Most of these counties had very little emissions from disturbances and hence not much post-disturbance growth. The slightly positive net fluxes in the Swain, Jackson, and Macon Counties were likely due to slightly higher disturbances towards the end of study period.

## 4. Discussion

The BCA model provides a useful tool for estimating carbon pools and fluxes arising from land use/land cover change. It has been used to calculate carbon estimates at national and global scales. However, because the smallest modeling unit of the model is an ecozone, it is difficult to use it to derive estimates with sub-ecozone details. To address this limitation, we reimplemented the BCA model within a gridded framework. The resultant grid-based carbon accounting (GCA) model provides a flexible framework for integrating remote sensing products into the carbon accounting process to produce spatially disaggregated carbon estimates, which are increasingly needed to support fine scale carbon management decision making and related applications.

As with the original BCA model, the estimates produced by the GCA model are attributed to different pools and change processes at an annual time step. While the BCA model has been widely used to estimate carbon fluxes arising from historical land use changes (Houghton et al. 1999, 2012; Houghton 2003b; Houghton and Nassikas 2017), the GCA model is intended for modeling the carbon dynamics of forest changes that occurred in recent decades during which key datasets such as disturbance history, land use conversion, and carbon density could be mapped using RS data. The sensitivity analysis conducted in this study demonstrated the need for reliable, fine resolution remote sensing data products for accurate estimation of carbon fluxes arising from contemporary forest disturbances and post-disturbance recovery. Large differences were found between the carbon estimates derived based on RS products and those derived using parameter values of the original BCA model, which were fine tuned for modeling historical land use changes.

Compared to estimates derived by assuming the forests had a mature forest carbon density value and all disturbances were stand clearing events, the carbon release from wood harvesting was reduced by more than 30% and 60%, respectively, when RS based disturbance intensity and carbon density data were used in deriving those estimates, and by more than 75% when both were used. As a result, the net flux arising from the observed disturbances and post-disturbance growth in North Carolina changed from 242.9 MT (source) to −47.2 MT (sink) when the disturbance intensity and pre-disturbance carbon density values used by the original BCA model were replaced by values derived based available fine resolution RS products.

Given the large impact of both forest carbon and disturbance intensity on carbon flux estimates, it is critically important to map these attributes with sufficient accuracy and adequate spatial and temporal details. While methods have been developed for producing forest disturbance products at the 30 m spatial resolution on an annual basis, forest carbon maps over large areas are available only for very few years (Wilson et al., 2013). Due to forest growth, the carbon value from a map developed for a specific year in general should not be used directly as the pre-disturbance carbon for calculating carbon emissions from a disturbance event that occurred in a different year. Annual forest carbon density maps would allow proper determination of the pre-disturbance carbon for disturbances that occurred in any year of the study domain. In the absence of such annual products, we developed an alternative method to create a pre-disturbance carbon density map based on a map produced for a specific year. The average values from the derived map were much closer to pre-disturbance carbon values measured by FIA field crew, demonstrating that the method we developed could be used to derive pre-disturbance carbon estimates in the absence of more reliable data.

Like any other science data, RS products, including those used in this study, typically have varying levels of uncertainties. However, as RS technology advances rapidly and increasingly more and better calibration data are becoming available, more RS products with better quality and quantified uncertainties will be developed. The gridded framework of the GCA model allows rapid integration of these new products to improve carbon estimation. This framework can be adapted for use with new, finer resolution remote sensing products as they become available.

It should be noted that GCA model implemented in this study only tracks the carbon accumulated through growth after a disturbance event. It does not calculate carbon changes from growth for the years before the first disturbance was detected over a pixel location, nor does it do so over forest areas that have no detected disturbances. In addition, other disturbance agents, such as insect or disease as well as major hurricanes are not considered. Although currently any disturbances not identified as fire or urban conversion are categorized as harvesting, in actuality the disturbance/recovery pattern of these additional disturbance types should be different from that of harvesting. While we intend to add modules to track these carbon changes in our future studies, the carbon estimates derived through this study do not provide a complete picture of forest carbon dynamics over North Carolina, and hence should not be used as evidence as to whether harvesting reduces or enhances carbon sequestration. More comprehensive experiments are needed to address this important question.

## 5. Conclusions

We have reimplemented the BCA model within a gridded framework to allow it to ingest fine resolution remote sensing products and produce carbon estimates with spatial details beyond the smallest modeling unit of the original BCA model. The resultant grid-based carbon accounting (GCA) model has been calibrated/parameterized such that it produces the same results as the original BCA model when the inputs to both models are equivalent. As with the original BCA model, the GCA model calculates carbon fluxes between major carbon pools arising from several disturbance types and post-disturbance growth over forestlands, including timber harvesting, fire, and conversion to urban area.

An important feature of the GCA model is that it can integrate fine resolution remote sensing products into the carbon accounting process to produce spatially disaggregated carbon estimates, which are increasingly needed to support fine scale carbon management decision makings and related applications. In North Carolina, the model was used to estimate carbon fluxes arising from forest disturbances mapped using historical Landsat observations over 1986–2010 to take advantage of their fine spatial resolution of 30 m and their consistent long-term record. The net flux from those disturbances and post-disturbance growth over the study period was 242.9 MT (source) when derived based on the original parameter values of the BCA model, which were tuned for modeling fluxes from historical land use change over several centuries. The flux was reduced to −47.2 MT (sink) when remote sensing-based disturbance attribution, disturbance intensity, as well as pre-disturbance carbon density products were used as model inputs, demonstrating that use of newly available fine resolution remote sensing products could have large impact on modeling the carbon fluxes arising from forest disturbance and post-disturbance growth. Therefore, improved estimates of those fluxes will rely heavily on further improving RS products using better observations and more accurate and more representative calibration data. Currently, the GCA model only tracks the carbon accumulated through growth after a disturbance event. Future efforts should focus on developing modules for calculating carbon changes from growth for the years before the first disturbance was detected over a pixel location, as well as growth over forest areas that have no detected disturbances, which is needed to provide a more complete picture of forest carbon dynamics.

## Declaration of competing interest

The authors declare that they have no known competing financial interests or personal relationships that could have appeared to influence the work reported in this paper.

## Acknowledgement

This study was made possible by NASA's Carbon Cycle Science and Land Cover and Land Use Change Programs (grant# NNX14AM39G, NNX14AD89G, and NNX15AE79G), the Laboratory of Environmental Model and Data Optima (EMDO, grant# 2106313), and Pie-Australia (grant# 19102901). Additional support was provided by the Department of Geographical Sciences of the University of Maryland. Elizabeth Burrill and Justin Holgerson of the US Forest Service assisted with the access to the FIA plot data, which was made possible through special agreements with the FIA program. We thank Dr. Jack (Jianguo) Ma for his long-term support.

## References

Agrawal, A., Nepstad, D., Chhatre, A., 2011. Reducing emissions from deforestation and forest degradation. Annu. Rev. Environ. Resour. 36, 373–396.

Antonarakis, A.S., 2014. Uncertainty in initial forest structure and composition when predicting carbon dynamics in a temperate forest. Ecol. Model. 291, 134–141. https://doi.org/10.1016/j.ecolmodel.2014.07.030.

Bardon, R.E., Megalos, M.A., New, B., Brogan, S., 2010. North Carolina's Forest Resources Assessment. NC Division of Forest Resources, Raleigh, North Carolina, p. 489.

Birdsey, R.A., Heath, L.S., 1995. Carbon changes in U.S. forests. In: Joyce, L.A. (Ed.), Productivity of America's Forests and Climate Change. Colorado USDA Forest Service, Fort Collins, pp. 56–70.

Birdsey, R., Pregitzer, K., Lucier, A., 2006. Forest carbon management in the United States. J. Environ. Qual. 35 (4), 1461–1469. https://doi.org/10.2134/jeq2005.0162.

Brack, C.L., Richards, G.P., 2002. Carbon accounting model for forests in Australia. Environ. Pollut. 116, S187–S194.

Bradford, J.B., Weishampel, P., Smith, M.-L., Kolka, R., Birdsey, R.A., Ollinger, S.V., Ryan, M.G., 2010. Carbon pools and fluxes in small temperate forest landscapes: variability and implications for sampling design. For. Ecol. Manag. 259, 1245–1254.

Brown, M.J., New, B.D., Johnson, T.G., Chamberlain, J.L., 2014. North Carolina's Forests, 2007. USDA-Forest Service, Southern Research Station, Asheville, NC, p. 112. Resour. Bull. SRS-RB-199.

Canadell, J.G., Raupach, M.R., 2008. Managing forests for climate change mitigation. Science 320, 1456–1457.
Crevoisier, C., Shevliakova, E., Gloor, M., Wirth, C., Pacala, S., 2007. Drivers of fire in the boreal forests: data constrained design of a prognostic model of burned area for use in dynamic global vegetation models. J. Geophys. Res. Atmos. 112 (24) https://doi.org/10.1029/2006JD008372.
DeFries, R.S., Houghton, R.A., Hansen, M.C., Field, C.B., Skole, D., Townshend, J., 2002. Carbon emissions from tropical deforestation and regrowth based on satellite observations for the 1980s and 1990s. Proc. Natl. Acad. Sci. U. S. A 99 (22), 14256–14261. https://doi.org/10.1073/pnas.182560099.
Denise, G., S, M.A., Stephen, C., 2011. Forest carbon management and carbon trading: a review of Canadian forest options for climate change mitigation. For. Chron. 87, 625–635.
Eidenshink, J., Schwind, B., Brewer, K., Zhu, Z.-L., Quayle, B., Howard, S., 2007. A project for monitoring Trends in Burn severity. Fire Ecol. 3, 3–21.
Fahey, T.J., Woodbury, P.B., Battles, J.J., Goodale, C.L., Hamburg, S.P., Ollinger, S.V., Woodall, C.W., 2010. Forest carbon storage: ecology, management, and policy. Front. Ecol. Environ. 8, 245–252.
Fan, S., Gloor, M., Mahlman, J., Pacala, S., Sarmiento, J., Takahashi, T., Tans, P., 1998. A large terrestrial carbon sink in North America implied by atmospheric and oceanic carbon dioxide data and models. Science 282, 442–446.
Friedlingstein, P., O'Sullivan, M., Jones, M., Andrew, R., Hauck, J., Olsen, A., et al., 2021. Global carbon budget 2021. Earth Syst. Sci. Data Discuss. (November), 1–3. https://doi.org/10.5194/essd-2021-386.
Goward, S.N., Masek, J.G., Cohen, W., Moisen, G., Collatz, G.J., Healey, S., Houghton, R., Huang, C., Kennedy, R., Law, B., Powell, S., Turner, D., Wulder, M.A., 2008. Forest disturbance and North American carbon flux. Eos Transact. 89, 105–116.
Goward, S.N., Huang, C., Masek, J.M., Cohen, W., Moisen, G., Nemani, R., 2010. US Forest Disturbance History from Landsat. National Aeronautics and Space Administration, p. 44.
Gray, A.N., Whittier, T.R., 2014. Carbon stocks and changes on Pacific Northwest national forests and the role of disturbance, management, and growth. For. Ecol. Manag. 328, 167–178. https://doi.org/10.1016/j.foreco.2014.05.015.
Griscom, B.W., Adams, J., Ellis, P.W., Houghton, R.A., Lomax, G., Miteva, D.A., Schlesinger, W.H., Shoch, D., Siikamäki, J.V., Smith, P., Woodbury, P., Zganjar, C., Blackman, A., Campari, J., Conant, R.T., Delgado, C., Elias, P., Gopalakrishna, T., Hamsik, M.R., Herrero, M., Kiesecker, J., Landis, E., Laestadius, L., Leavitt, S.M., Minnemeyer, S., Polasky, S., Potapov, P., Putz, F.E., Sanderman, J., Silvius, M., Wollenberg, E., Fargione, J., 2017. Natural climate solutions. Proc. Natl. Acad. Sci. Unit. States Am. 114, 11645–11650.
Hall, R.J., Skakun, R.S., Arsenault, E.J., Case, B.S., 2006. Modeling forest stand structure attributes using Landsat ETM+ data: application to mapping of aboveground biomass and stand volume. For. Ecol. Manag. 225 (1–3), 378–390. https://doi.org/10.1016/j.foreco.2006.01.014.
Homer, C., Dewitz, J., Yang, L., Jin, S., Danielson, P., Xian, G., Coulston, J., Herold, N., Wickham, J., Megown, K., 2015. Completion of the 2011 national land cover database for the conterminous United States – representing a decade of land cover change information. Photogramm. Eng. Rem. Sens. 81, 345–354.
Houghton, R.A., Hackler, J.L., Lawrence, K.T., 1999. The U.S. carbon budget: contributions from land-use change. Science 285, 574–578.
Houghton, R.A., 2003a. Why are estimates of the terrestrial carbon balance so different? Global Change Biol. 9, 500–509.
Houghton, R.A., 2003b. Revised estimates of the annual net flux of carbon to the atmosphere from changes in land use and land management 1850-2000. Tellus Ser. B Chem. Phys. Meteorol. 55, 378–390.
Houghton, R.A., House, J.I., Pongratz, J., van der Werf, G.R., DeFries, R.S., Hansen, M.C., Le Quere, C., Ramankutty, N., 2012. Carbon emissions from land use and land-cover change. Biogeosciences 9, 5125–5142.
Houghton, R.A., 2013. Keeping management effects separate from environmental effects in terrestrial carbon accounting. Global Change Biol. 19 (9), 2609–2612. https://doi.org/10.1111/gcb.12233.
Houghton, R.A., Nassikas, Alexander A., 2017. Global and regional fluxes of carbon from land use and land cover change 1850–2015. AGU:Glob. Biogeochem. Cycles 456–472.
Huang, C., Goward, S.N., Masek, J.G., Gao, F., Vermote, E.F., Thomas, N., Schleeweis, K., Kennedy, R.E., Zhu, Z., Eidenshink, J.C., Townshend, J.R.G., 2009. Development of time series stacks of Landsat images for reconstructing forest disturbance history. Int. J. Digi. Earth 2, 195–218.
Huang, C., Goward, S.N., Masek, J.G., Thomas, N., Zhu, Z., Vogelmann, J.E., 2010. An automated approach for reconstructing recent forest disturbance history using dense Landsat time series stacks. Remote Sens. Environ. 114, 183–198.
Huang, C., Ling, P.-Y., Zhu, Z., 2015. North Carolina's forest disturbance and timber production assessed using time series Landsat observations. Int. J. Digi. Earth 8, 947–969.
Huntzinger, D.N., Post, W.M., Wei, Y., Michalak, A.M., West, T.O., Jacobson, A.R., Baker, I.T., Chen, J.M., Davis, K.J., Hayes, D.J., Hoffman, F.M., Jain, A.K., Liu, S., McGuire, A.D., Neilson, R.P., Potter, C., Poulter, B., Price, D., Raczka, B.M., Tian, H. Q., Thornton, P., Tomelleri, E., Viovy, N., Xiao, J., Yuan, W., Zeng, N., Zhao, M., Cook, R., 2012. North American Carbon Program (NACP) regional interim synthesis: terrestrial biospheric model intercomparison. Ecol. Model. 232, 144–157.
Hurtt, G.C., Pacala, S.W., Moorcroft, P.R., Caspersen, J., Shevliakova, E., Houghton, R.A., Moore, B., 2002. Projecting the future of the U.S. carbon sink. Proc. Natl. Acad. Sci. Unit. States Am. 99 (3), 1389–1394. https://doi.org/10.1073/pnas.012249999.
IPCC, 2014. AR5 Synthesis Report: Climate Change 2014. IPCC. https://www.ipcc.ch/report/ar5/syr/.
Jenkins, J.C., Chomnacky, D.C., Heath, L.S., Birdsey, R.A., 2003. National scale biomass estimators for United States tree species. For. Sci. 49, 12–35.
Kellndorfer, J., Walker, W., LaPoint, E., Cormier, T., Bishop, J., Fiske, G., Kirsch, K., 2013. Vegetation Height, Biomass, and Carbon Stock for the Conterminous United States: A High-Resolution Dataset from Landsat ETM+, SRTM-InSAR, National Land Cover Database, and Forest Inventory and Analysis Data Fusion.
Kuemmerle, T., Olofsson, P., Chaskovskyy, O., Baumann, M., Ostapowicz, K., Woodcock, C.E., et al., 2011. Post-Soviet farmland abandonment, forest recovery, and carbon sequestration in western Ukraine. Global Change Biol. 17 (3), 1335–1349. https://doi.org/10.1111/j.1365-2486.2010.02333.x.
Lamb, R.L., Hurtt, G.C., Boudreau, T.J., Campbell, E., Sepúlveda Carlo, E.A., Chu, H.-H., de Mooy, J., Dubayah, R.O., Gonsalves, D., Guy, M., Hultman, N.E., Lehman, S., Leon, B., Lister, A.J., Lynch, C., Ma, L., Martin, C., Robbins, N., Rudee, A., Silva, C.E., Skoglund, C., Tang, H., 2021. Context and future directions for integrating forest carbon into sub-national climate mitigation planning in the RGGI region of the U.S. Environ. Res. Lett. 16, 063001.
Le Quéré, C., Andrew, R.M., Canadell, J.G., Sitch, S., Ivar Korsbakken, J., Peters, G.P., et al., 2016. Global carbon budget 2016. Earth Syst. Sci. Data 8 (2), 605–649. https://doi.org/10.5194/essd-8-605-2016.
Marland, G., Pielke, R.A., Apps, M., Avissar, R., Betts, R.A., Davis, K.J., Frumhoff, P.C., Jackson, S.T., Joyce, L.A., Kauppi, P., Katzenberger, J., MacDicken, K.G., Neilson, R. P., Niles, J.O., Niyogi, D.d.S., Norby, R.J., Pena, N., Sampson, N., Xue, Y., 2003. The climatic impacts of land surface change and carbon management, and the implications for climate-change mitigation policy. Clim. Pol. 3, 149–157.
Noormets, A., Epron, D., Domec, J.C., McNulty, S.G., Fox, T., Sun, G., King, J.S., 2015. Effects of forest management on productivity and carbon sequestration: a review and hypothesis. For. Ecol. Manag. 355, 124–140.
Pacala, S.W., Hurtt, G.C., Baker, D., Peylin, P., Houghton, R.A., Birdsey, R.A., Heath, L., Sundquist, E.T., Stallard, R.F., Ciais, P., Moorcroft, P., Caspersen, J.P., Shevliakova, E., Moore, B., Kohlmaier, G., Holland, E., Gloor, M., Harmon, M.E., Fan, S.M., Sarmiento, J.L., Goodale, C.L., Schimel, D., Field, C.B., 2001. Consistent land- and atmosphere-based U.S. Carbon sink estimates. Science 292, 2316–2320.
Pan, Y., Birdsey, R.A., Fang, J., Houghton, R., Kauppi, P.E., Kurz, W.A., Phillips, O.L., Shvidenko, A., Lewis, S.L., Canadell, J.G., Ciais, P., Jackson, R.B., Pacala, S., McGuire, A.D., Piao, S., Rautiainen, A., Sitch, S., Hayes, D., 2011. A large and persistent carbon sink in the world's forests. Science 333, 988–993.
Powell, S.L., Cohen, W.B., Healey, S.P., Kennedy, R.E., Moisen, G.G., Pierce, K.B., Ohmann, J.L., 2010. Quantification of live aboveground forest biomass dynamics with Landsat time-series and field inventory data: a comparison of empirical modeling approaches. Remote Sens. Environ. 114, 1053–1068.
Santi, E., Paloscia, S., Pettinato, S., Fontanelli, G., Mura, M., Zolli, C., et al., 2017. The potential of multifrequency SAR images for estimating forest biomass in Mediterranean areas. Remote Sens. Environ. 200 (July), 63–73. https://doi.org/10.1016/j.rse.2017.07.038.
Schleeweis, K.G., Moisen, G.G., Schroeder, T.A., Toney, C., Freeman, E.A., Goward, S.N., Huang, C., Dungan, J.L., 2020. US national maps attributing forest change: 1986–2010. Forests 11 (6), 653.
Schroeder, T.A., Healey, S.P., Moisen, G.G., Frescino, T.S., Cohen, W.B., Huang, C., Yang, Z., 2014. Improving estimates of forest disturbance by combining observations from landsat time series with U.S. Forest Service Forest Inventory and Analysis data. Remote Sens. Environ. 154 (1), 61–73. https://doi.org/10.1016/j.rse.2014.08.005.
Schulze, E.D., Valentini, R., Sanz, M.J., 2002. The long way from Kyoto to Marrakesh: implications of the Kyoto Protocol negotiations for global ecology. Global Change Biol. 8, 505–518.
Smith, B.W., Miles, P.D., Perry, C.H., Pugh, S.A., 2007. Forest Resources of the United States: a Technical Document Supporting the Forest Service 2010 RPA Assessment. General Techincal Report. U.S. Department of Agriculture, Forest Service, Washington Office, Washington, D.C.
Tang, X., Hutyra, L.R., Arévalo, P., Baccini, A., Woodcock, C.E., Olofsson, P., 2020. Spatiotemporal tracking of carbon emissions and uptake using time series analysis of Landsat data: a spatially explicit carbon bookkeeping model. Sci. Total Environ. 720, 137409 https://doi.org/10.1016/j.scitotenv.2020.137409.
Tao, X., Huang, C., Zhao, F., Schleeweis, K., Masek, J., Liang, S., 2019. Mapping forest disturbance intensity in North and South Carolina using annual Landsat observations and field inventory data. Remote Sens. Environ. 221, 351–362.
Tian, H., Melillo, J.M., Kicklighter, D.W., McGuire, A.D., Helfrich, J., 1999. The sensitivity of terrestrial carbon storage to historical climate variability and atmospheric CO2 in the United States. Tellus Ser. B Chem. Phys. Meteorol. 51, 414–452.
Turner, D.P., Koerper, G.J., Harmon, M.E., Lee, J.J., 1995. A carbon budget for forests of the conterminous united-states. Ecol. Appl. 5, 421–436.
Turner, D.P., Ritts, W.D., Kennedy, R.E., Gray, A.N., Yang, Z., 2016. Regional carbon cycle responses to 25 years of variation in climate and disturbance in the US Pacific Northwest. Reg. Environ. Change 16 (8), 2345–2355. https://doi.org/10.1007/s10113-016-0956-9.
Williams, C.A., Hasler, N., Gu, H., Zhou, Y., 2020. Forest Carbon Stocks and Fluxes from the NFCMS, Conterminous USA. ORNL DAAC, Oak Ridge, Tennessee, USA, pp. 1990–2010. https://doi.org/10.3334/ORNLDAAC/1829.

Wilson, B.T., Woodall, C., Griffith, D., 2013. Imputing forest carbon stock estimates from inventory plots to a nationally continuous coverage. Carbon Bal. Manag. 8, 1.
Xiao, J., Chevallier, F., Gomez, C., Guanter, L., Hicke, J.A., Huete, A.R., et al., 2019. Remote sensing of the terrestrial carbon cycle: a review of advances over 50 years. Remote Sens. Environ. 233 (January), 111383 https://doi.org/10.1016/j.rse.2019.111383.
Zheng, D., Linda, S.H., Ducey, M.J., Smith, J.E., 2011. Carbon changes in conterminous US forests associated with growth and major disturbances: 1992-2001. Environ. Res. Lett. 6, 014012.